

INCREASING SOLAR PHOTOVOLTAIC EFFICIENCY USING TILT ANGLE OPTIMIZATION

ABDULLAHI YUSUF SADA¹

^{*1}Department of Electrical & Computer Engineering, Baze University, Abuja, Nigeria

Abstract - As energy demand increases with increase in population and urbanization, renewable energy sources are needed. These renewable energy sources unlike conventional sources of energy do not use up the natural resources available. They also produce considerably low levels of environmental pollutants and are continuously available. Renewable sources are not only preferred because of their availability and sustainability but also because of increasing energy cost and the need for replacement of ageing sources. Solar energy being the energy produced from sunlight can be extracted using solar panel electricity systems, also referred to as solar photovoltaics (PV). These PV panels capture the sun's energy by the use of photovoltaic cells which convert the energy into electricity. There is variation in the amount of solar energy captured by the cells caused by the effect of temperature and irradiance on the PV voltage and current. This also has affects the efficiency of the solar PV. Different methods have been used to obtain higher efficiency by adjusting or improving the components of the PV system. Even with these changes and improvements, if the actual solar irradiation is not utilized, the efficiency will not be at its peak. With regards to that, tilt angle optimization is used in this report to get the maximum solar radiation at any given time so the maximum efficiency of the solar PV can be achieved.

Keywords: Photovoltaic, Maximum Power Point Tracking (MPPT), Solar Radiation, Tilt Angle Optimization, Texas Instrument

I. INTRODUCTION

Daylight is converted to electricity cleanly, silently and safely with the use of photovoltaic (PV) system. The function of a PV is identical to that of a p-n junction. Using the effect known as photovoltaic effect, a solar cell does the conversion of light to electricity. The output of the solar cell is a direct current (DC). The size of the cell and the amount of light intensity determine the current produced while the semiconductor material used for the cell determines the voltage [1].

A solar cell's output is determined in terms of peak Watts (Wp) under international standard condition of 1KW/m² sunlight intensity. A single solar cell produces significantly low current. Solar cells are connected in series and then in parallel then covered with glass or plastic to form a module [2].

Important factors that affect the output solar PVs are atmospheric conditions. The atmospheric parameters that have effect on the PV efficiency include irradiance, temperature, wind speed, dust and installation conditions [3]. The temperature of the module is another parameter that affects the

performance of a PV system because it modifies system efficiency and output.

Increase in atmospheric temperature tends to result in voltage drops while decrease in temperature results in higher voltages. Irradiance on the other hand affects the output current of the PV system as its increase results in higher current and its decrease results in lower current. Dust can possibly accumulate on the surface of the PV module thereby preventing sunlight hitting the panel and decrease the output [4].

Due to the effects of so many factors on the PV system, this paper aims at providing possible solutions on how to maximize the efficiency of solar PV systems through tilt angle optimization.

1.1 Solar Explorer Kit

This kit provides a flexible and low voltage platform to assess the C2000 microcontroller family of devices for variation of solar applications [5]. As the PV panel is a DC source with non-linear current-voltage characteristics, it is important to always extract maximum power from the panel by operating at the MPP of this non-linear current-voltage characteristics and convert the power so it can be used to charge energy saving devices, operate DC loads, operate AC loads, or supply power to an existing electrical grid.

Based on the requirements of a system, different types of power topologies can be applied. The Texas Instruments C2000 microcontroller family, which has an enhanced outlying set and optimized CPU core for control objectives, is ideal for these power control applications.

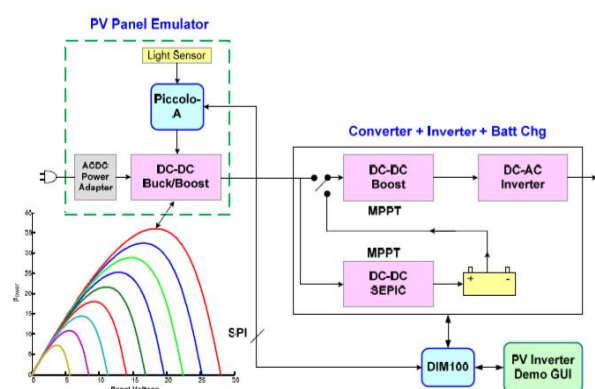


Figure 1: Solar Explorer Kit Overview

The kit has an input voltage of 20V and a DC power supply which powers the controller and existing motherboard. It can be connected to a PV panel with a rated power of 50W. It also contains a PV emulator power stage along with other stages which can be used to assess power from the panel. The PV panel's control is separated from the control of the other power stages.

The kit makes use of two C2000 controllers, the first is a Piccolo-A device used for the control of the PV emulator stage. While the other is a single c2000 device which uses a control-card that controls all other power stages like, DC-DC Boost stage, DC-AC and DC-DC Sepic stage. The control-card can be placed in the DIMM100 slot on the board.

As solar PV highly depends on light, a light sensor is available which can be used to change the behavior of the panel under different lighting conditions.

1.2 Solar Angles

As the earth rotates around its axis every 24 hours and makes an annual revolution around the sun, it is tilted to an angle of 23.45 degrees to the elliptic plane as shown in Figure 2 below [9].

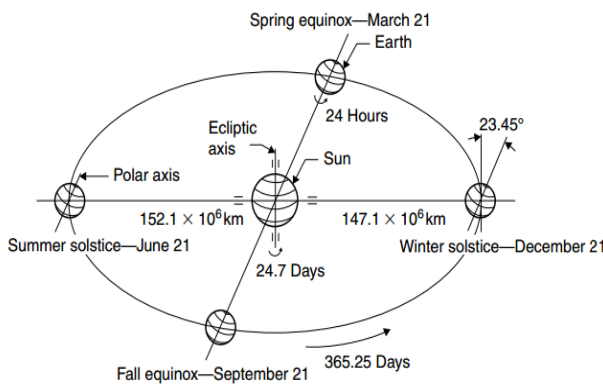


Figure 2: Annual motion of the earth about the sun [7]

To accurately predict the location of the sun for solar applications, two astronomical angles can be used to determine its position with respect to an observer on earth. The solar altitude angle (α) and solar azimuth (z).

1.2.1. Declination Angle (δ)

This is the included angle of the line connecting Earth's core to that of the sun and the equatorial plane of Earth. Its value varies yearly and changes daily. The respective variation range is $\pm 23^\circ 27'$ [10]. When the declination is towards the north, it is positive.

Figure 3 shows the variation of declination from spring to winter equinox

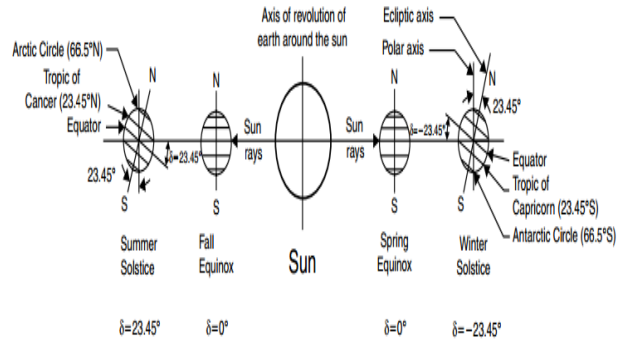


Figure 3: Yearly variation of solar declination [31]

This variation for any day of the year (N) can be calculated using the equation below:

$$\delta = 23.45 \sin\left(\frac{360}{365}(284 + N)\right) \tag{1}$$

1.2.2 Hour Angle (h)

The hour angle of a position on the surface of the earth is the position to which the earth would rotate to make the meridian be at a point directly under the sun [11]. At noon, the solar angle is zero and each 15 degrees of latitude determines one hour which makes afternoon hours are positive. This angle can be determined using apparent solar time (AST) with the equation below.

$$h = (AST - 12)15 \tag{2}$$

1.2.3 Solar Altitude Angle (α)

This is the angle between the rays of the sun and a horizontal plane. It is derived in terms of solar zenith angle (Φ) which is the angle between the rays of the sun and the vertical [12].

$$\Phi + \alpha = \frac{\pi}{2} = 90^\circ \tag{3}$$

The solar altitude can be calculated using:

$$\sin(\alpha) = \cos(\Phi) = \sin(L) \sin(\delta) \cos(h) \tag{4}$$

Where L is the local latitude described as the angle between a line from earth's centre to the site of interest and the equatorial plane.

1.2.4 Solar Azimuth Angle (z)

This is the angle of the rays of the sun measured in the horizontal plane from due south for Northern Hemisphere and due north for Southern Hemisphere [12]. Cranfield University is in the Northern hemisphere. The azimuth angle can be calculated using:

$$\tan(z) = \frac{\sin(h)}{\sin(L) \cos(h) - \cos(L) \tan(\delta)} \tag{5}$$

1.2.5 Incidence Angle (θ)

This is the angle between the rays of the sun and normal surface. The incidence angle is equal to the zenith angle for a horizontal plane. The angle of incidence for south-facing tilted surfaces in the Northern Hemisphere is expressed as

$$\begin{aligned} \cos(\theta) = & \sin(L)\sin(\delta)\cos(\beta) \\ & - \cos(L)\sin(\delta)\sin(\beta) \\ & + \cos(L)\cos(\delta)\cos(h)\cos(\beta) \\ & + \sin(L)\cos(h)\sin(\beta) \end{aligned} \quad (6)$$

Where Z_s is the surface azimuth angle and β is surface tilt angle from the horizontal. For horizontal surfaces, when $\beta = 0^\circ$, $\theta = \Phi$

1.3 Solar Radiation

[7] defined solar constant (G_{sc}) as the amount of solar energy per unit time, at the mean distance of the earth from the sun, received on a unit area of surface normal to the sun outside the atmosphere. When the sun is closest to the earth which is at January 3rd, the solar constant is 1400W/m^2 and 1330W/m^2 when the sun is farthest away from the earth, July 4th.

1.3.1 Extra-terrestrial Radiation

The extra-terrestrial radiation measured on a plane which is normal to the radiation on any day of the year, G_{on} , varies between $1330 - 1400\text{W/m}^2$ at a range of 3.3% and it can be calculated by

$$G_{on} = G_{sc} \left(1 + 0.033 \cos\left(\frac{360N}{365}\right) \right) \quad (7)$$

The rate of solar radiation when a surface is placed parallel to the ground, G_{oH} , incident on extra-terrestrial horizontal surface can be calculated as

$$\begin{aligned} G_{oH} = & G_{on} * \cos(\Phi) \\ = & G_{sc} \left(1 + 0.033 \cos\left(\frac{360N}{365}\right) \right) \\ & * (\cos(L)\cos(\delta)\cos(h) \\ & + \sin(\delta)) \end{aligned} \quad (8)$$

Total radiation, H_o , incident on an extra-terrestrial horizontal surface in the period of a day can be calculated

$$\begin{aligned} H_o = & \frac{24 * 3600 G_{sc}}{\pi} * \left(1 + 0.033 \cos\left(\frac{360N}{365}\right) \right) \\ & * (\cos(L)\cos(\delta)\sin(h_{ss}) \\ & + \left(\frac{\pi h_{ss}}{180}\right) \sin(L)\sin(\delta)) \end{aligned} \quad (9)$$

The correlation for calculating the monthly average daily total global radiation on a horizontal surface, H_g is given by

$$\frac{H_g}{H_o} = a + b \left(\frac{n}{N} \right) \quad (10)$$

Where the coefficients a and b are the empirical coefficients and are said to be 0.23 and 0.48 respectively. These values are applicable for all the locations in the world according to [20].

The monthly average daily diffuse correlation can be obtained using an expression given by [8]

$$\begin{aligned} & \text{For } h_{ss} \leq 81.4^\circ \text{ and } 0.3 \leq K_T \leq 0.8 \\ & \frac{H_D}{H_g} = 1.391 - 3.560K_T + 4.189K_T^2 - 2.137K_T^3 \\ & \text{For } h_{ss} \geq 81.4^\circ \text{ and } 0.3 \leq K_T \leq 0.8 \\ & \frac{H_D}{H_g} = 1.311 - 3.022K_T + 3.427K_T^2 - 1.821K_T^3 \end{aligned}$$

Where H_g is the monthly average daily total radiation and H_D is the monthly average diffuse radiation. With these values obtained, the monthly average beam radiation can be calculated using

$$H_B = H_g - H_D \quad (13)$$

1.3.2 Transparent Plates

For a transparent plate, when a beam of radiation hits the surface at a certain angle θ_1 , referred to as the incidence angle, some of the radiation reflects and the rest refracts to an angle θ_2 known as the refraction angle as shown in Figure 4.

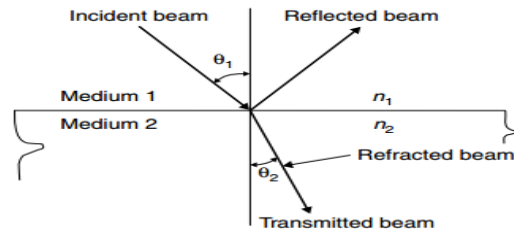


Figure 4: Incident and Refraction Angles for beam passing from a medium.

These two angles are related using Snell's law:

$$n = \frac{n_1}{n_2} = \frac{\sin(\theta_1)}{\sin(\theta_2)} \quad (14)$$

Where n_1 and n_2 are the indices of refraction while n is the ratio of refraction index. The refraction index has a typical value of 1.000 for air, 1.526 for glass and 1.33 for water.

The equations for parallel and perpendicular parameters of radiation for smooth surfaces are as follows

$$r_{\perp} = \frac{\sin^2(\theta_2 - \theta_1)}{\sin^2(\theta_2 + \theta_1)} \quad (15)$$

$$r_{\parallel} = \frac{\tan^2(\theta_2 - \theta_1)}{\tan^2(\theta_2 + \theta_1)} \quad (16)$$

The transmittance for reflection losses, τ_r , can be derived using the equation below

$$\tau_r = \frac{1}{2} \left(\frac{1 - r_{\parallel}}{1 + r_{\perp}} + \frac{1 - r_{\perp}}{1 + r_{\parallel}} \right) \quad (1)$$

The transmittance for absorption losses, τ_a , can be derived by the equation below

$$\tau_a = e^{-\frac{KL}{\cos\theta_2}} \quad (18)$$

Where K is the coefficient of extinction that ranges from 4m^{-1} for glass with low quality and 32m^{-1} for glass with high quality, and L is the glass cover thickness.

The reflectance of one cover can be obtained by

$$\rho = \tau_a(1 - \tau_r) \quad (19)$$

The ratio of total average beam radiation for a month, R_b , for surfaces in the northern hemisphere is given by Yadav et al. is

$$R_b = \frac{\cos(L - \beta) \cos(\delta) \sin(h) + \left(\frac{\pi}{180}\right) h \sin(L - \beta) \sin(\delta)}{\cos(L) \cos(\delta) \sin(h) + \left(\frac{\pi}{180}\right) h \sin(L) \sin(\delta)} \quad (20)$$

The diffuse radiation conversion factor, R_d , is given by

$$R_d = \frac{1 - \cos\beta}{2} \quad (21)$$

Ground reflected radiation conversion factor, R_r , is calculated by

$$R_r = \rho * \frac{1 - \cos\beta}{2} \quad (22)$$

With all the coefficients calculated, the monthly average for daily radiation on an inclined surface for a particular day of the month using:

$$H_T = H_g \left(\left(1 - \frac{H_D}{H_g}\right) R_b + \frac{H_D}{H_g} R_d + R_r \right) \quad (23)$$

II. SIMULATION

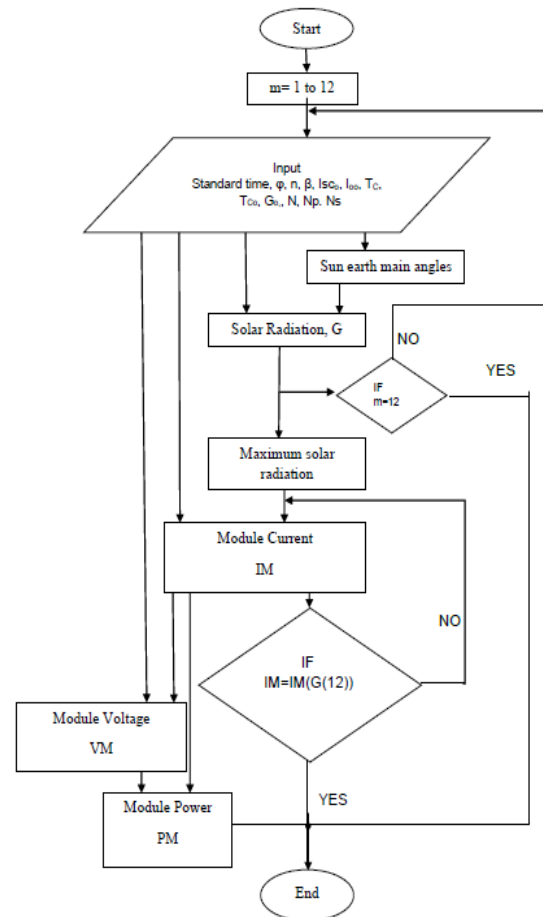


Figure 5: Flow Chart of Simulation

The flow chart shows how the simulation operates to obtain maximum efficiency with monthly average optimum tilt angle. Maximum efficiency in this application is based on the power output of the PV module.

First, the month (m) needs to be specified and the standard parameters which include nominal operation conditions, number of cells, bright sunshine hours, ideality factor of the diode and latitude angle. This latitude angle is specifically important as it is used to specify the exact location of the PV module which is Cranfield University (52° North). The solar angles are then calculated using the latitude angle, solar time and number of days. The solar radiation is a function of the geographical location and solar angles.

This procedure is applied to all the months of the year and the tilt angle changes from $0 - 90^\circ$ from the horizontal plane. The simulation code is able to identify the maximum solar irradiance that is obtained with optimum tilt angle. This maximum solar irradiance is then used to compute the I-V and P-V characteristics of the PV module.

III. RESULT AND DISCUSSION

To understand the efficiency of the PV panel different conditions were formulated by covering some cells on the PV panel and the readings were recorded and plotted. A load test was also carried out to observe how different duty cycles of the PWM affect the system.

From the simulation, different tilt angles were tried for each month and plotted to obtain the optimum radiation. Also, the power for each month is plotted. These plots will be compared and discussed in this paper.

The solar PV panel used contains 36 monocrystalline silicon cells with a rated power of 50W, open-circuit voltage of 22.83V and short-circuit current of 2.94A under 1000W/m² of solar radiation and 25°C of cell temperature. These parameters were included in simulation and were run to obtain figures 6 & 7 below.

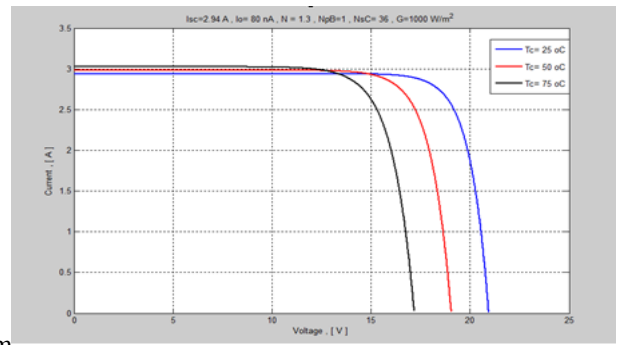
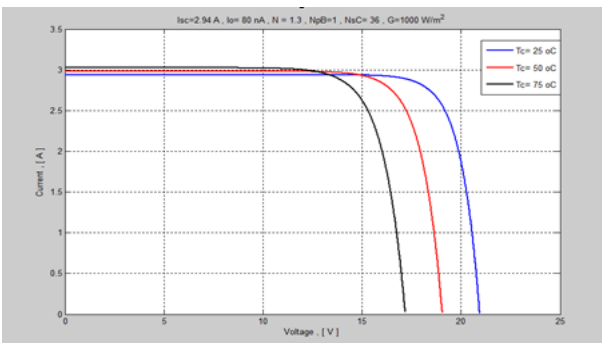


Figure 6: I-V Curve for Solar PV



From Figure &

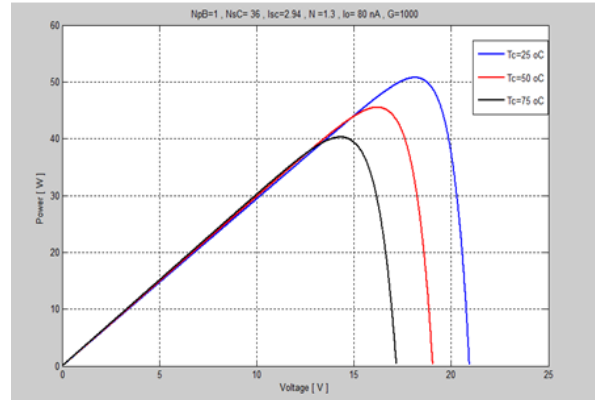


Figure 7: P-V curve for Solar PV

Figure which were obtained from the simulation, the output current, voltage and power are similar to that of the PV panel's ideal condition so this proves the simulation can be used to assume certain situations of the PV panel.

3.1.1 Sunny Condition

In this case, the solar panel was placed outside when the skies were clear and the light was not obstructed by the clouds. The readings were recorded for different tilt angles.

Table 1 below shows the readings obtained at around 1pm on Thursday 17th July, 2014.

Table 1: Sunny Condition

Sunny Condition					
x	y	Angle (Deg)	Voltage	Current	Power
0	0	0	13.72	2.65	36.52
62	24	21.16	13.74	2.88	39.55
58	32	28.89	13.46	2.86	38.21
52	44	40.24	13.39	2.75	36.66
49	49	45.00	13.75	2.66	36.71
44	54	50.83	13.95	2.53	35.33
36	58	58.17	13.74	2.47	33.92
		90.00	15.43	1.53	23.44

From

Table 1 above, it can be seen that the optimum tilt angle at 1pm is 21.16deg where the maximum power is obtained. This is as a

result of the location of the sun. As the angle increases, the power decreases. At 90deg, when the panel is not directed to the sun at all, the power drops significantly. The current also drops as result of the reduced solar intensity while the voltage increased.

3.1.2 Cloudy Condition

In this case, the readings were taken when the skies were cloudy. Like the previous case, the tilt angles were adjusted and the current, voltage and power were recorded.

Table 2 below shows the obtained results. Also from the simulation, different levels of irradiation were applied and variable results were obtained.

Table 2: Cloudy Condition

Cloudy Condition					
x	y	Angle (Deg)	Voltage	Current	Power
0	0	0	15.41	0.72	11.07
62	24	21.16	15.61	0.85	13.28
58	32	28.89	14.6	0.89	12.98
52	44	40.24	14.71	0.84	12.36
49	49	45.00	14.8	0.86	12.67
44	54	50.83	14.77	0.76	11.23
36	58	58.17	14.83	0.69	10.21
		90.00	15.19	0.47	7.13

From the table above, the optimum tilt angle is found to be the same as the previous case but the current and voltage vary, hence the power varies too.

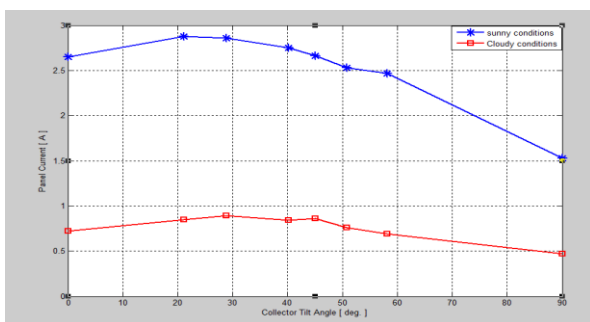


Figure 8: Current Plot

From figure 8 above, it can be seen that the current is much higher in the sunny case. This is due to the fact that the amount of irradiance greatly affects the level of current produced from the PV panel. So as the sun was shaded by the clouds, the current produced dropped.

The figure below shows the two voltage outputs of both cases.

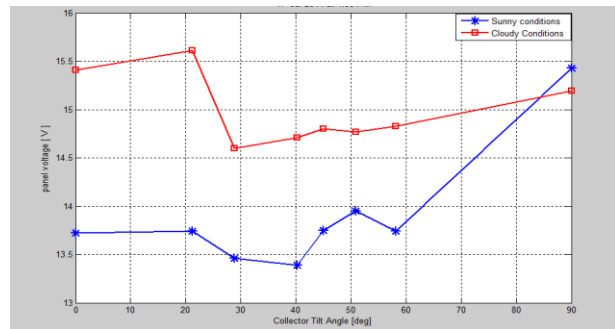


Figure 9: Voltage Plots

From figure 9 above, the voltage is slightly higher during the cloudy condition. This has to do with the slight drop in temperature as irradiance generally has very little effect on the voltage output.

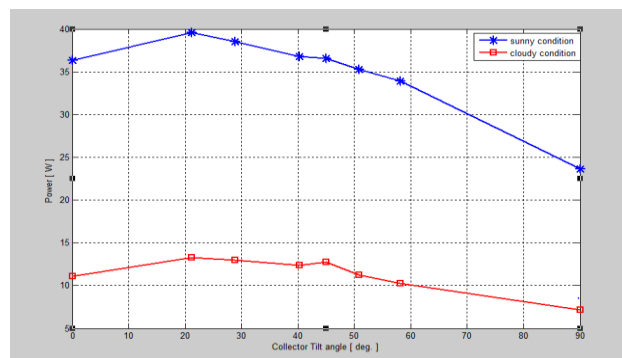


Figure 10: Power plot

Figure 10 above shows the plot of power for both cases and it can be observed that the power is much higher in during the sunny condition. As the current is much higher during the sunny condition, this shows that current has more effect on the power produced. So the best output that can be obtained from the PV panel is during the sunny condition.

3.1.3 Partial Shading

This case was carried out to observe the sensitivity of the solar PV. A number of cells from different sides of the panel were covered to see which part of the panel is more sensitive to changes.

Table 3: Partial Shading

Partial Shading				
No of Cells Shaded	% Covered	V	I	P
0	0	14.37	2.43	34.10
3TR	8.33	19.08	0.23	4.41
3TL		19.09	0.17	3.27

3BR		18.97	0.18	3.41
3BL		18.94	0.18	3.33
6TR	16.67	18.44	0.15	2.77
6TL		18.06	0.14	2.46
6BR		17.52	0.15	2.65
6BL		18.74	0.15	2.64
9TR		25	16.70	0.14
9TL	15.08		0.14	2.20
9BR	15.77		0.14	2.23
9BL	18.20		0.13	2.33
18L	50		17.43	0.10
18R		17.53	0.11	2.27

From table 3 above, the terms TR, TL, BR & BL stan for top right, top left, bottom left & bottom right respectively. It can be seen that as the number of cells covered increases, the out power and current decreases. This is as a result of the high effect of irradiance on produced current. The voltage on the other hand increased as 3 cells were covered because of the effect of temperature on the voltage produced. But as the number of cells covered increased, the voltage decreased slightly due to the little effect irradiance has on the voltage.

The huge drop of current after covering the cells does show that the cells in the module are connected in series. Because when cells are connected series and a cell in the connection is blocked, this cuts of the connection between cells and thereby prevents most of the current from flowing.

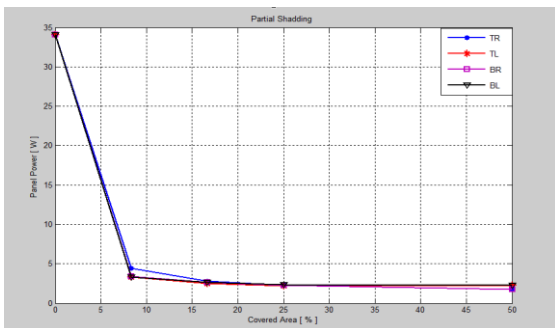


Figure 11: Power Plots for Partial Shading

Figure shows that regardless of which part of the panel is covered, the output is approximately the same.

3.1.4 Load Test

A 24VDC motor with 4000rpm was used as the load. Different duty cycle of the PWM were used to observe how it affects the output and performance of the motor. As shown in figure 33 & 34 below, as the duty cycle of the PWM increases, the frequency and RPM also increase until the optimum duty cycle is reached, which is 0.6. But beyond the optimum point, the frequency and RPM decrease with increasing duty cycle. The load current also increases because there is direct relationship between load current and RPM.

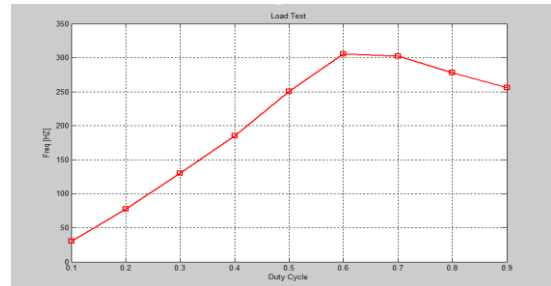


Figure 12: Effect of Duty Cycle on Frequency

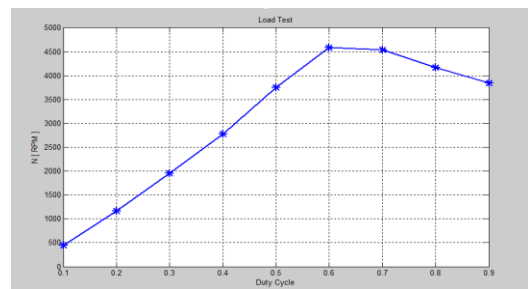


Figure 13: Effect of Duty Cycle on RPM

Also comparing the Figure which was gotten on the 17th of July, 2014 and table 4 which was recorded on the 30th of July, 2014, it can be seen that the optimum duty cycle is 0.6 and an RPM of 4545.

IV. CONCLUSION

Efficiency of the solar PV can be increased through different methods. The type of solar cell used, the MPPT technique used, design of the system based on an application, the type of power converter used also helps improve efficiency.

The most important factor affecting solar PV efficiency is the level of irradiance. With little or no irradiance, there will be very low efficiency. Hence the positioning of the solar panel is particularly important. The optimum tilt angle and direction needs to be used to obtain the maximum efficiency at all times. Depending on the time of the year and location, the position of the sun and its availability varies.

The simulation designed to calculate the output of the solar PV module using optimum tilt angle ran successfully. Using the simulation, the optimum tilt angle for every month of the year in Cranfield, United Kingdom was obtained.

The solar explorer kit was used to experiment on a solar panel with monocrystalline silicon cells existing on Cranfield campus. The experiments were carried out successfully and all the intended objectives were achieved.

V. REFERENCES

- [1] Vidyanandan, K. V. (2017). An overview of factors affecting the performance of solar PV systems. *Energy Scan*, 27, 2-8.
- [2] Riverola, A., Vossier, A., & Chemisana, D. (2019). Fundamentals of solar cells. In *Nanomaterials for Solar Cell Applications* (pp. 3-33). Elsevier.
- [3] Perraki, V., & Kounavis, P. (2016). Effect of temperature and radiation on the parameters of photovoltaic modules. *Journal of Renewable and Sustainable Energy*, 8(1), 013102.
- [4] Andrea, Y., Pogrebnaya, T., & Kichonge, B. (2019). Effect of industrial dust deposition on photovoltaic module performance: Experimental measurements in the tropical region. *International Journal of Photoenergy*, 2019.
- [5] Bhardwaj, M., & Subharmanya, B. (2013). PV inverter design using Solar Explorer Kit. *Texas Instruments Incorporated*, 19-20.
- [6] Ghazi, S., & Ip, K. (2014). The effect of weather conditions on the efficiency of PV panels in the southeast of UK. *Renewable energy*, 69, 50-59.
- [7] Soteris K. (2009) "Solar Energy Engineering- Processes and Systems", *Copyright@ Elsevier Inc.*
- [8] Erbs, D. G., Klein, S. A., & Duffie, J. A. (1982). Estimation of the diffuse radiation fraction for hourly, daily and monthly-average global radiation. *Solar energy*, 28(4), 293-302.
- [9] Kalogirou, S. A. (2012). *Solar thermal systems: Components and applications-introduction*. Elsevier Ltd.
- [10] Wang Z. (2019). Chapter 2 - The Solar Resource and Meteorological Parameters, *Design of Solar Thermal Power Plants*, Academic Press, 47-115,
- [11] Page, J. (2012). The Role of Solar-Radiation Climatology in the Design of Photovoltaic Systems. *Practical Handbook of Photovoltaics*, 573–643.
- [12] Soteris A. K. (2014). Chapter 2 - Environmental Characteristics, *Solar Energy Engineering (Second Edition)*, Academic Press, 51-123
- [13] Iqbal, M. (2012). *An introduction to solar radiation*. Elsevier.
- [14] Pernía, A. M., Arias, J., Prieto, M. J. and Martínez, J. Á. (2009), "A modular strategy for isolated photovoltaic systems based on microcontroller", *Renewable Energy*, vol. 34, no. 7, pp. 1825-1832.



Abdullahi Sada holds a bachelor's degree in Electrical & Control Engineering and a Master's degree in Renewable Energy Engineering. His research interests are in Control, Renewable Energy Systems, Energy Efficiency & Power Systems Reliability.